Int. J. Electrochem. Sci., 15 **(2020)** 1606 – 1621, doi: 10.20964/2020.02.46

International Journal of
ELECTROCHEMICAL
SCIENCE
www.electrochemsci.org

Polystyrene Sulfonic Acid-Doped Polypyrrol (dppy) as a Corrosion Inhibitor for Carbon Steel in 1.0 M HCl Solution

Xiumei Wang[*], *Jiani Xing*

School of Materials Science and Engineering, Shenyang Jianzhu University, Shenyang, Liaoning, China 110168
[*]E-mail: xmwang@alum.imr.ac.cn

Received: 18 October 2019 / *Accepted:* 8 December 2019 / *Published:* 31 December 2019

The inhibition performance of doped polypyrrol (dppy) for carbon steel corrosion in 1.0 M HCl solution was investigated and analyzed by weight loss method, electrochemical techniques and SEM micrographs. The results denote that both the concentration of dppy and the experimental temperature enhance the inhibitive efficiency, and the highest inhibitive efficiency is 87.1% at 40 mg L^{-1} (333 K) based on the weight loss results. Dppy hinders both anodic and cathodic processes simultaneously by removing water molecules through stronger adsorption, and the self-corrosion potential (*E*) exhibits almost no change with the increasing dppy concentration, suggesting dppy is a mixed-type corrosion inhibitor. Dppy is adsorbed on the carbon steel surface by mixed physisorption and chemisorption. The dppy adsorption conforms to the Langmuir isotherm model, and the adsorption is a spontaneous, endothermic process with an increase in entropy.

Keywords: Corrosion Inhibitor; Doped Polypyrrol (dppy); Carbon Steel; 1.0 M HCl Solution; Electrochemical Technique

1. INTRODUCTION

Carbon steel is extensively employed in a large number of industrial fields owing to its low cost and excellent performance, but it is inevitably subject to different degrees of corrosion in its applied environments [1-2]. Acid corrosion of carbon steel is an extremely prominent problem that plagues industrial development, such as pipeline boiler system pickling and descaling, chemical cleaning, and acidification of oil and gas wells [3]. Among many anticorrosion methods, corrosion inhibitors have been widely used and played important roles because of their good economy, high inhibition effect and excellent adaptability. The organic components used as corrosion inhibitors usually contain an electronegative atom such as N, O, S, etc., which can provide a lone pair of electrons, a double bond, a triple bond, or a large conjugate system that is capable of providing π

electrons [4-8]. These structural features of the compound molecules can act as active centers to provide or accept electrons, interact with metal surface atoms and adsorb on the metal surface to form an adsorption film, separating the metal surface from the corrosive medium to achieve corrosion inhibition. Generally, the central N atom of an organic compound with N atom has an unpaired electron pair and can form a coordination bond with the empty d-orbital of the metal, so the molecules are adsorbed on the metal surface to form a protective film, thereby suppressing the corrosion of metal [9-15].

Polypyrrole contains a pyrrole ring capable of providing a plurality of π electrons and N atom capable of providing a lone pair of electrons, which structurally conforms to the requirements of corrosion inhibitor molecules. However, polypyrrole has poor solubility and can only be dissolved in a small amount of high boiling organic solvents. To date, there are few reports on polypyrrole as a corrosion inhibitor. A large number of studies on the anticorrosion mechanism have been focused on polypyrrole coating [16-22].

At present, with the in-depth study of the polypyrrole polymerization process, the solubility has been effectively improved, and it has become possible to prepare water-soluble polypyrrole. Therefore, studying the corrosion inhibition performance of water-soluble polypyrrole on metals will expand the application range of polypyrrole in the anticorrosion field. In this paper, we synthesized doped polypyrrole (dppy) and evaluated the corrosion protection of doped polypyrrole on carbon steel in 1.0 M HCl solution through weight loss measurements, electrochemical impedance spectroscopy (EIS) techniques, potentiodynamic polarization tests and SEM micrographs.

2. EXPERIMENTAL

2.1 Synthesis of doped polypyrrol (dppy)

Prior to use, the pyrrole (py, Aldrich, 99%) was vacuum-distilled and stored at 4℃. Ammonium persulfate ($(NH_4)_2S_2O_8$, APS) was used as the oxidant and polystyrene sulfonic acid (PSSA) as the doping acid. Dppy powders with different molar ratios of py/PSSA were prepared by controlling pyrrole monomer at a certain ratio with APS and adjusting PSSA amount. The samples were numbered by 1~5# (1:0.3, 1:0.5, 1:1, 1:2 and 1:6, respectively). The solubility of dppy increased with PSSA amount (65.0% for 1:0.3, 86.3% for 1:0.5, 94.2% for 1:1, 98.7% for 1:2 and 98.7% for 1:6). The solubility reached a maximum value 98.7% at 1:2 molar ratio of py/PSSA. However, the solubility showed no obvious change with further increase of molar ratio of py/PSSA (1:6). The polymerization process of doped polypyrrole(1:2 molar ratios of py/PSSA) is as follows: 4.0 mmol PSSA was added to 20 mL of deionized water, and was sonicated and completely dissolved; then the solution was transferred into a flask kept at 0-5℃ in an ice water bath; Next, 2.0 mmol of the above pyrrole was added to 10 mL deionized water, and sonicated to dissolve and form a homogeneous solution, which was slowly added to the flask dropwise, and stirred at 0 to 5 ℃ for 1 h. 10 mL (0.2 mol/L) of ammonium persulfate was added dropwise to the above system for 2 h, and the entire reaction lasted for 12 h. The reaction was stopped and a black emulsion was obtained, was demulsified with acetone, filtered, and washed three times with deionized water and absolute ethanol. A black

product was obtained and dried in a vacuum drying oven for 5 h at 60℃. This dppy was studied as a corrosion inhibitor for carbon steel without any further treatment. The concentration of dppy is expressed as a mass concentration (10, 20, 30, and 40 mg L^{-1}).

2.2 Weight loss measurements

The weight loss measurements were performed by employing cuboid carbon steel samples (purity, 99.99%, 30 mm × 15 mm ×15 mm), and one surface was marked by number. The surface of the sample was polished by $100^{\#}$, $200^{\#}$, $400^{\#}$, $600^{\#}$ and $800^{\#}$ water sanding paper sequentially, washed with deionized water, cleaned by ultrasonic waves and degreased in absolute ethanol, dried in a desiccator for 24 hours, and weighed with an analytical balance with an accuracy ± 0.1mg. The size of each carbon steel specimen was measured accurately with a vernier caliper to calculate the surface area of the carbon steel specimen exposed in the corrosive medium. Then the numbered surface of each carbon steel sample was sealed with a waterproof glue.

The carbon steel samples were immersed in 1.0 M HC1 media containing various concentration of corrosion inhibitor (dppy), and 1.0 M HC1 solution without corrosion inhibitor (dppy) was used as a blank control. The experimental temperature ranged from 303K to 333 K controlled by thermostatic water bath, the volume of the acid was 200 mL, and the immersion duration was 5 h. The samples were taken out, rinsed with running water, cleaned surface corrosion products by a brush, washed with deionized water, dehydrated in anhydrous ethanol, dried with N_2 gas, waterproof glue was removed from the surface, scrubbed with absolute ethanol, and then dried in a desiccator for 24 h. In order to obtain reliable data on the weight loss results, three parallel carbon steel samples were suspended in 1.0 M HC1 solution without and with any concentration of dppy and an average corrosion rate was achieved. The corrosion rate (V), inhibitive efficiency (η_W), and surface coverage (θ) were acquired using the following Eqs(1), (2), and (3):

$$V = \frac{\Delta W}{S \times t} \qquad (1)$$

$$\eta_W\% = \frac{V^0 - V^{inh}}{V^0} \times 100\% \qquad (2)$$

$$\theta = \frac{V^0 - V^{inh}}{V^0} \qquad (3)$$

Wherein, ΔW was the weight loss of carbon steel sheet (g), A was the immersion surface area (m^2), t was the immersion time (h), θ was the surface coverage, $V°$ and V^{inh} were the average corrosion rates of carbon steel sheet (g m^{-2} h^{-1}) in the absence and presence of dppy, respectively.

2.3 Electrochemical measurements

The material for the electrochemical tests was the same as that for the weight loss test, and the electrode size was 10mm×10mm ×10 mm. Except for the working surface (10 mm × 10 mm), the other

surfaces of the electrode were encapsulated with epoxy resin, and the working surfaces were polished with $100^{\#}$, $200^{\#}$, $400^{\#}$, $600^{\#}$, and $800^{\#}$ water sanding paper in a stepwise manner. The surfaces were washed with deionized water, cleaned by an ultrasonic wave cleaner and degreased with acetone to serve as a working electrode. PARSTAT2273 electrochemical workstation (USA) and a three-electrode system were applied to conduct the electrochemical experiments. A carbon steel electrode was employed as the working electrode, a platinum electrode (20 mm × 20 mm) and a saturated calomel electrode (SCE) were used as an auxiliary electrode and a reference electrode, respcetively. The measured potentials in the electrochemical experiments were as a reference to the SCE scale. The open-circuit potential (OCP) in different corrosion media was monitored for 1800 seconds until the open circuit potential (OCP) was stable; that was, the OCP fluctuated below 2 mV within 5min before electrochemical measurement. The potentiodynamic polarization curves were conducted in ± 250mV versus OCP at a 2mV s^{-1} scan rate, the data was analyzed by Powersuite software. The electrochemical impedance spectroscopy (EIS) data were acquired by applying a sinusoidal voltage with 10 mV amplitude in the frequency range from 100kHz to 10mHz at the steady-state open-circuit potential(OCP). The EIS data analysis was performed using Zsimpwin. To acquire reliable and reproducible results, a fresh working electrode was used in each run and three runs were conducted for each test.

2.4 Scanning electron microscopy (SEM)

Carbon steel sheets with a size of 30 mm × 15 mm × 15 mm were polished with $100^{\#}$, $200^{\#}$, $400^{\#}$, $600^{\#}$, and $800^{\#}$ water sanding paper gradually, washed with deionized water, degreased with acetone, and dried. The samples were suspended in a blank 1.0 M HCl solution and 1.0 M HCl with 40 mg L^{-1} dppy for 5 h at 303 K. Then, the test sample was taken out, and the surface of the sample was rinsed with deionized water and anhydrous ethanol respectively, finally dried in desiccator for 12h. The surface morphology of the sample after corrosion was analyzed by a *Hitachi* S-4800 scanning electron microscope, and the acceleration voltage was 15 kV.

3 RESULTS AND DISCUSSION

3.1 Weight loss results

The effect of dppy concentration and temperature on corrosion inhibition and corrosion rate of carbon steel in 1.0 M HCl solution at 303K is displayed in Figure 1 and Figure 2. It can be seen from Figure 1 and Figure 2 that dppy has a certain inhibitory effect on carbon steel in 1.0 M HC1 solution at any concentration and temperature, and the corrosion inhibitive efficiency of dppy increases with the increase of concentration and temperature, while corrosion rate decreases with the increment in dppy concentration and the reduction in temperature. When dppy concentration reaches 40 mg L^{-1} at any temperature, the corrosion inhibition efficiency reaches the highest value, exceeding 80% (80.6% at

303K, 81.9% at 313K, 83.6% at 323K, 87.1% at 333K), which can be considered as an excellent corrosion inhibitor.

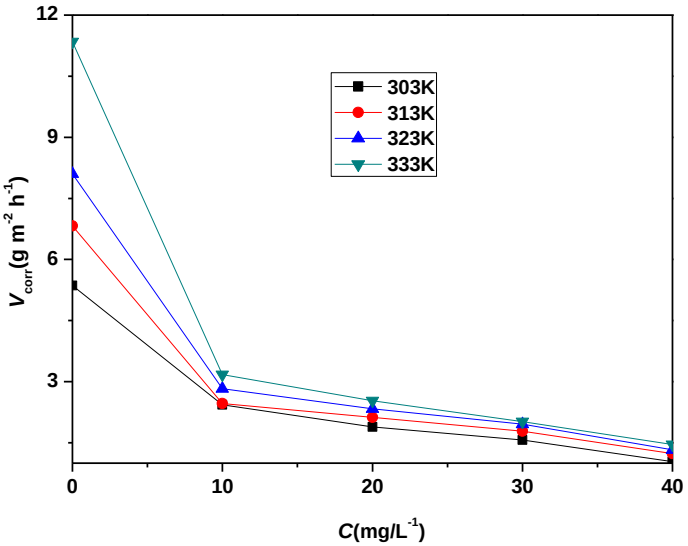

Figure 1. The corrosion rate of carbon steel in 1.0 M HCl solution as a function of dppy concentration and temperature.

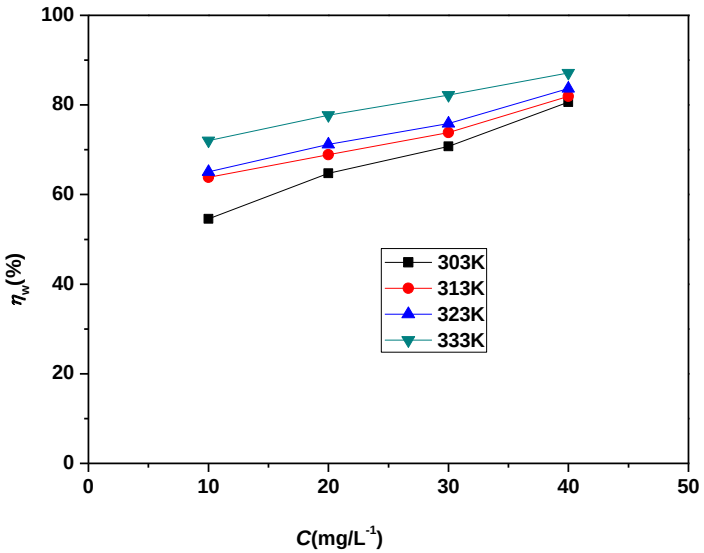

Figure 2. The variation of corrosion inhibitive efficiency η_w with dppy concentration and temperature.

Generally, the inhibitive efficiency is considered to decrease with the increase in temperature, while the inhibitive efficiency of dppy increases with the temperature. This phenomenon indicates that there may be a strong chemical interaction by charge transferring or electron sharing between dppy molecules and empty d-orbital of carbon steel. A similar report was previously published [23]. Here, it must be emphasized that the higher corrosion efficiency was acquired merely on the basis of a stronger

increase in the corrosion rate value with increasing temperature in the blank 1.0 M HCl solution compared to the inhibited 1.0 M HCl solution.

3.2 Electrochemical Impedance Spectroscopy (EIS)

The Nyquist diagrams of the carbon steel electrode in 1.0 M HCl solution without and with the addition of various concentrations of dppy are shown Figure 3.

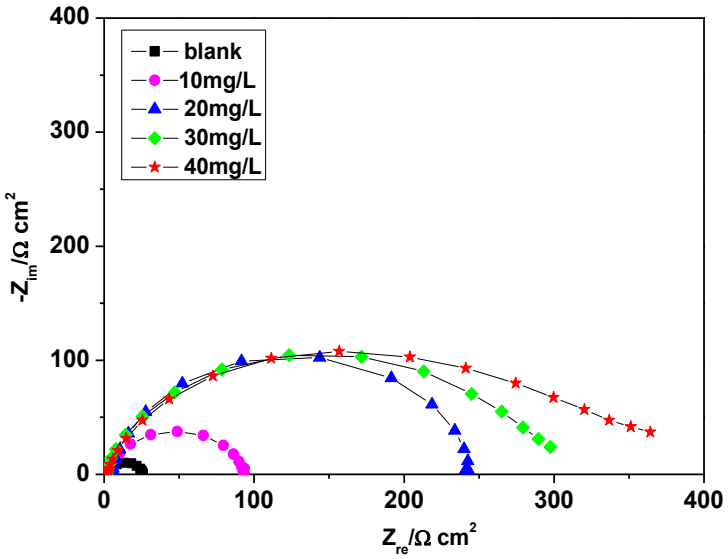

Figure 3. Impedance response of carbon steel in 1.0 M HCl solution in the absence and presence of various concentrations of dppy at 303K.

It can be seen in Figure 3 that the Nyquist plots of the carbon steel electrodes at all dppy concentration are mainly composed of a single semicircular arc in the tested frequency range, this response is the result of charge transfer in the solution [24-25]. The depressed and imperfect semicircular shape of the capacitive loop could be caused by inhomogeneities and roughness on the carbon steel electrode surface, uneven distribution of the surface active sites and the adsorption of the dppy on the carbon steel surface.

The impedance characteristics of the carbon steel electrode are changed drastically by the addition of dppy. The size of the capacitive loop enhanced with increment in dppy concentration, especially at high concentrations. This increase was marked with the increase of dppy concentration, denoting the inhibition efficiency is dependent on the dppy concentration [26]. The increase in the dppy concentration accelerates the interaction rate between dppy molecules and the carbon steel at the active sites resulting in more adsorption and higher surface coverage on the carbon steel electrode surface [27-28].

After analyzing the impedance spectra, an equivalent electrochemical circuit [29] (depicted in Figure 4) was applied to fit the Nyquist plot data and the obtained parameters are shown in Table 1.

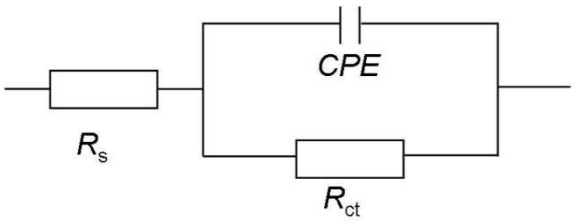

Figure 4. Equivalent circuit to fit the experimental data.

The R_s represents the solution resistance, CPE_{dl} represents the double layer constant phase angle element at the interface between the carbon steel electrode and solution, R_{ct} is the charge-transfer resistance, and the corrosion inhibitive efficiency η_R is acquired from the obtained charge transfer resistance R_{ct}. The calculation formula of corrosion inhibitive efficiency η_R is shown as equation (4):

$$\eta_R\% = \frac{R_{ct}^{inh} - R_{ct}^{o}}{R_{ct}^{inh}} \times 100\% \qquad (4)$$

where $R_{ct}{}^{o}$and $R_{ct}{}^{inh}$ are the charge transfer resistances of the carbon steel electrode in 1.0 M HCl solution without and with dppy, respectively.

In order to obtain high accuracy, *CPE* as a substituent for a pure capacitor is applied to fit the impedance diagrams of carbon steel electrode [30-31]. The impedance of *CPE* is calculated by equation (5) [32]:

$$Z_{CPE} = Y_0^{-1}(j\omega)^{-n} \qquad (5)$$

where Y_o is the magnitude of *CPE, j* is the square root of −1, ω is the angular frequency and n is the phase shift. The double layer capacitance $(CPE)_{dl}$ was obtained by equation (6):

$$CPE_{dl} == \frac{Y\omega R^{n-1}}{\sin(n(\frac{\pi}{2}))} \qquad (6)$$

As shown in Table 1, R_{ct} increased greatly after dppy was added to the corrosive solution and continuously increased with the increment of dppy concentration resulting in enhanced inhibitive efficiency. The result is ascribed to the formation of dppy adsorption film on carbon steel electrode surface. The adsorption film acts as a barrier to protect carbon steel by separating the carbon steel electrode from the corrosive solution thereby suppressing more charge and mass transfer. When the dppy concentration is increased to 40 mg L^{-1}, the corrosion inhibitive efficiency is further increased to 92.3%. Compared with general organic corrosion inhibitors [33-34], only a small amount of dppy is needed to achieve a higher corrosion inhibition efficiency. Additionally, Y_o for the double layer reduces with the increment in dppy concentration. The increase in R_{ct} and the reduction in Y_o may be assigned to dppy displacing a great number of water molecules on the carbon steel electrode subsequently decreasing significantly the active sites that are necessary for the occurrence of corrosion [35]. The phase shift, *n*, values show no significant change in all the corrosive solutions. The stable *n*

value for the double layer suggests that the mechanism of carbon steel dissolution is dominated by charge transfer with and without dppy.

The drastic decrease in the Y_o at higher dppy concentrations is owing to dppy adsorbed on the carbon steel electrode making charged species inaccessible to the carbon steel surface [36]. This could be illustrated that the formed dppy protective film hinders the corrosive solution from attacking the carbon steel electrode [37-38].

Table 1. Electrochemical parameters obtained by EIS.

		CPE_{dl}			
C_{inh}	R_s	Y_o	n	R_{ct}	η_R
/mg L^{-1}	/Ω cm^2	/μΩ s^n cm^{-2}		/Ω cm^2	/%
blank	2.2	825	0.91	20	-
10	2.9	467	0.90	93	78.5
20	2.0	239	0.92	236	91.5
30	1.7	187	0.91	309	93.5
40	2.1	92	0.90	382	94.0

3.3 Potentiodynamic polarization curves

Figure 5 shows the potentiodynamic polarization curves of a carbon steel electrode in 1.0 M HCl solution without and with various concentrations of dppy. The relevant electrochemical parameters (corrosion current density (i) and the self-corrosion potential (E) obtained by extrapolation) are listed in Table 2. The corrosion inhibitive efficiency η_i is obtained using the following formula [39].

$$\eta_i\% = \frac{i^0 - i^{inh}}{i^0} \times 100\% \qquad (7)$$

where $i^0$and i^{inh} are the corrosion current densities of carbon steel electrodes in 1.0 M HCl media without and with dppy, respectively.

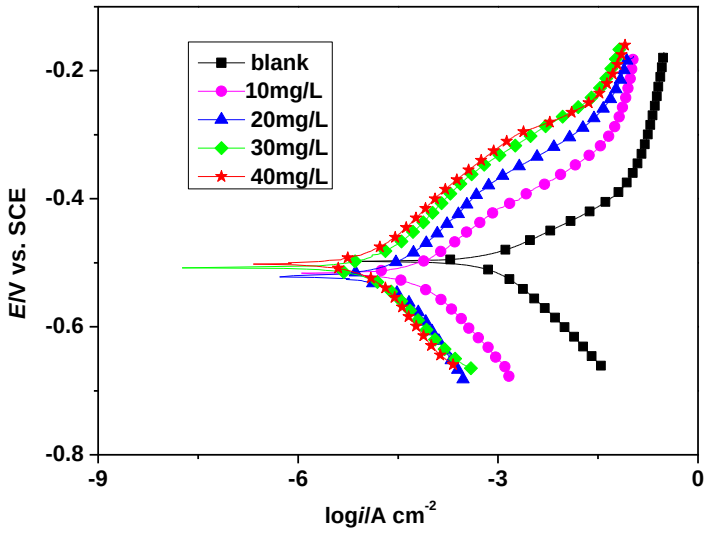

Figure 5. Potentiodynamic polarization curves of carbon steel electrode in 1.0 M HCl solution without and with addition of various concentration of dppy at 303 K.

Table 2. The relevant parameters acquired by extrapolation of potentiodynamic polarization curves and calculated η_i%.

C_{inh} /mg L^{-1}	-*E* /V vs SCE	*i* /×10^{-5}A cm^{-2}	η_i /%
blank	0.504	17	-
10	0.515	5.4	68.2
20	0.520	2.8	83.5
30	0.508	1.6	90.6
40	0.502	1.2	92.9

It is shown in Figure 5 that the shape of the anodic and cathodic branches of the carbon steel electrode in HCl media with different concentrations of dppy has no obvious change, which is basically parallel to that in HCl without dppy, but the corrosion current densities for the cathodic and anodic polarization curves shift to significantly lower values with the increasing dppy concentration. It is obvious that dppy behaves as a mixed-type inhibitor simultaneously slowing down both the anodic carbon steel oxidation and the cathodic hydrogen ion reduction reactions. These results are in agreement with an inhibition mechanism induced by the geometric blocking of the carbon steel surface by the adsorbed particles with corrosion inhibition performance. In general, this geometric blocking effect results in a decrease in the active reaction area [40].

As can be listed in Table 2, the addition of dppy effectively decreased the corrosion current density (17×10^{-5} A cm^{-2} for blank, 1.2×10^{-5} A cm^{-2} for 40mg L^{-1}) and the corrosion inhibition efficiency was reached 92.9%, showing good corrosion inhibition performance. Meanwhile, it also can

be seen from Table 2 that the self-corrosion potential (*E*) of the carbon steel electrode in uninhibited and inhibited media shows no significant change which further proves that dppy is a mixed-type corrosion inhibitor[41].

3.4 Adsorption isotherm model

In general, the adsorption mode of corrosion inhibitor molecules on the surface of carbon steel to form a protective film can be well used to explain the inhibition mechanism of many inhibitors [42-46]. Physisorption and chemisorption are two basic modes of corrosion inhibitors.

The adsorption of inhibitors can be illustrated in detail using the adsorption isotherm model [47]. The data were fitted by different adsorption isotherm models (Langmuir isotherm, Frumkin isotherm, Temkin isotherm and Freundluich isotherm) [48]. It is shown the best fit for dppy is the Langmuir isotherm model, which is displayed as follows:

$$\frac{C_{\text{inh}}}{\theta} = C_{\text{inh}} + \frac{1}{K_{\text{ads}}} \quad (8)$$

where C_{inh} is the dppy concentration (mg L^{-1}), θ is the surface coverage (calculated from the weight loss results due to the characteristics of a mixed-type corrosion inhibitor), and K_{ads} is the adsorption equilibrium constant, L g^{-1}.

Introducing θ into the Langmuir adsorption isotherm and plotting C/θ versus C yields straight lines at different temperatures (Figure 6) with R^2 close to 1 and a slope near unity (Table 3). This phenomenon in which slope deviates from unity may be due to mutual repulsion or attraction forces between the dppy molecules adsorbed on the carbon steel surface [49-50]. The intercept obtained by fitting the plots of C/θ versus C is used to calculate the K_{ads} value at different temperatures and the corresponding results are as follows: 111.5, 173.7, 181.9 and 262.8 L g^{-1} for 303, 313, 323 and 333 K, respectively.

The adsorption Gibbs free energy ($\Delta G^{\text{o}}_{\text{ads}}$) can be obtained through K_{ads} by the related equation and listed in Table 3[51].

$$K_{\text{ads}} = \frac{1}{C_{\text{solvent}}} \exp\left(\frac{-\Delta G^{\text{o}}_{\text{ads}}}{RT}\right) \quad (9)$$

where R represents the molar gas constant, 8.314 J mol^{-1} K^{-1}; T represents the absolute temperature, K; C_{solvent} is the mass concentration of water, 1000 g L^{-1}, and $\Delta G^{\text{o}}_{\text{ads}}$ denotes the adsorption Gibbs free energy, kJ mol^{-1}.

It is well accepted that $\Delta G^{\text{o}}_{\text{ads}}$ plays an important role in explaining the adsorption process of corrosion inhibitors. Basically, the absolute value of $\Delta G^{\text{o}}_{\text{ads}}$ less than 20 kJ mol^{-1} is defined as physisorption while the value over 40 kJ mol^{-1} suggests electrons sharing or transferring from the inhibitor to the empty d-orbital of metal to form more stable coordinate bonds (chemisorption) [52-54]. The $\Delta G^{\text{o}}_{\text{ads}}$ values are found -29.3, -31.4, -32.5 and -34.6 kJ mol^{-1} at 303-333 K, respectively,

suggesting that the adsorption of dppy on the carbon steel surface is not a single physical adsorption or chemical adsorption, but a mixed-type adsorption dominated by chemical adsorption [55-56].

The standard adsorption enthalpy ΔH^{o}_{ads} can be acquired by the Van't Hoff formula [57]:

$$\ln K_{ads} = \frac{-\Delta H^{0}_{ads}}{RT} + B \qquad (10)$$

where K_{ads} denotes the adsorption equilibrium constant, L g^{-1}; R represents the molar gas constant, 8.314 J K^{-1} mol^{-1}; T represents the absolute temperature, K. B represents the integration constant. Plotting $\ln K_{ads}$ versus $1/T$ shows a straight line with high linear correlation coefficient (R^2=0.9978, close to 1) in Figure 7. The slope obtained by fitting the plot of $\ln K_{ads}$ versus $1/T$ is equal to $\Delta H^{o}_{ads}/R$ which is applied to achieve ΔH^{o}_{ads} as depicted in Table 3.

The standard adsorption entropy $\triangle S^{o}_{ads}$ can be calculated using $\triangle H^{o}_{ads}$ and $\triangle G^{o}_{ads}$ by formula (11) and is also shown in Table 3.

$$\Delta G_{ads}{}^{o} = \Delta H^{o}_{ads} - T \times \Delta S^{o}_{ads} \qquad (11)$$

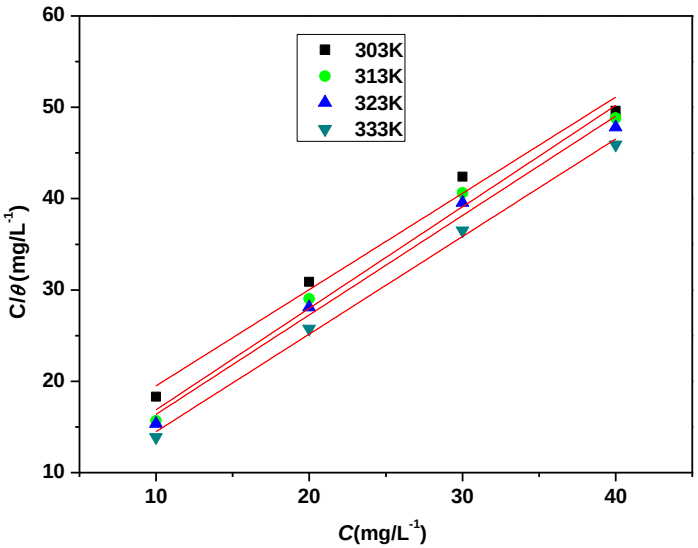

Figure 6. Langmuir isotherm adsorption model of dppy on the carbon steel surface in 1.0 M HCl solution at 303 - 333 K.

Table 3. Thermodynamic parameters obtained by fitting Langmuir isotherm adsorption model.

T /K	K_{ads} L g^{-1}	R^2	slope	$\Delta G°_{ads}$ /kJ mol^{-1}	$\Delta H°_{ads}$ /kJ mol^{-1}	$\Delta S°_{ads}$ /J mol^{-1} K^{-1}
303	111.5	0.97938	1.05365	-29.3	22.0	170
313	173.7	0.98356	1.11138	-31.4		171
323	181.9	0.98707	1.08837	-32.5		169
333	262.8	0.99600	1.06808	-34.6		171

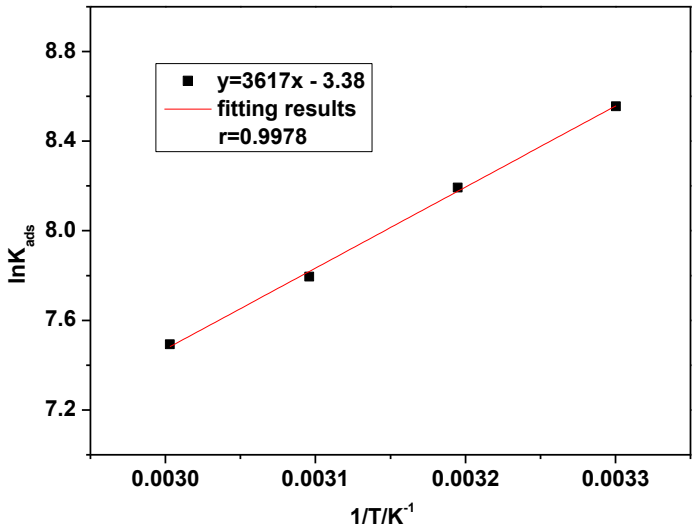

Figure 7. Straight line of ln K_{ads} versus 1/T from Van't Hoff equation.

It is well known the positive value of ΔH^{o}_{ads} represents an endothermic adsorption process suggesting corrosion inhibitive efficiency is enhanced by the increment in temperature at the same concentration. This result can be illustrated the increment in corrosion rate of carbon steel in the uninhibited medium is much faster than that in the inhibited medium. At the selected experimental temperatures, all $\triangle S^{o}_{ads}$ values are also positive and exhibit little change. This fact indicates that the adsorption of dppy is a process accompanied by an increase in entropy. The positive $\Delta H_{ads}{}^{o}$ value denotes that dppy molecules adsorption on the carbon steel surface is an endothermic process accompanied by chemisorption. This is a good explanation that corrosion inhibitive efficiency enhances with the rise of temperature in this work (weight loss results).

3.5 Scanning Electron Microscopy (SEM) Results

SEM micrographs of carbon steel sheets immersed in 1.0 M HCl solution without and with the addition of 40 mg L^{-1} dppy for 5 h are illustrated in Figure 8. As it is shown in Figure 8, the carbon steel surface without immersion in corrosive solution is relatively flat and smooth with no corrosion, but there are still regular scratches (Figure 8a).

The carbon steel surface suspended in blank 1.0 M HCl solution for 5 h (Figure 8b) shows a highly corroded and uneven surface with a great number of pits. However, there was a significant reduction in carbon steel corrosion with the addition of 40 mg L^{-1} dppy.

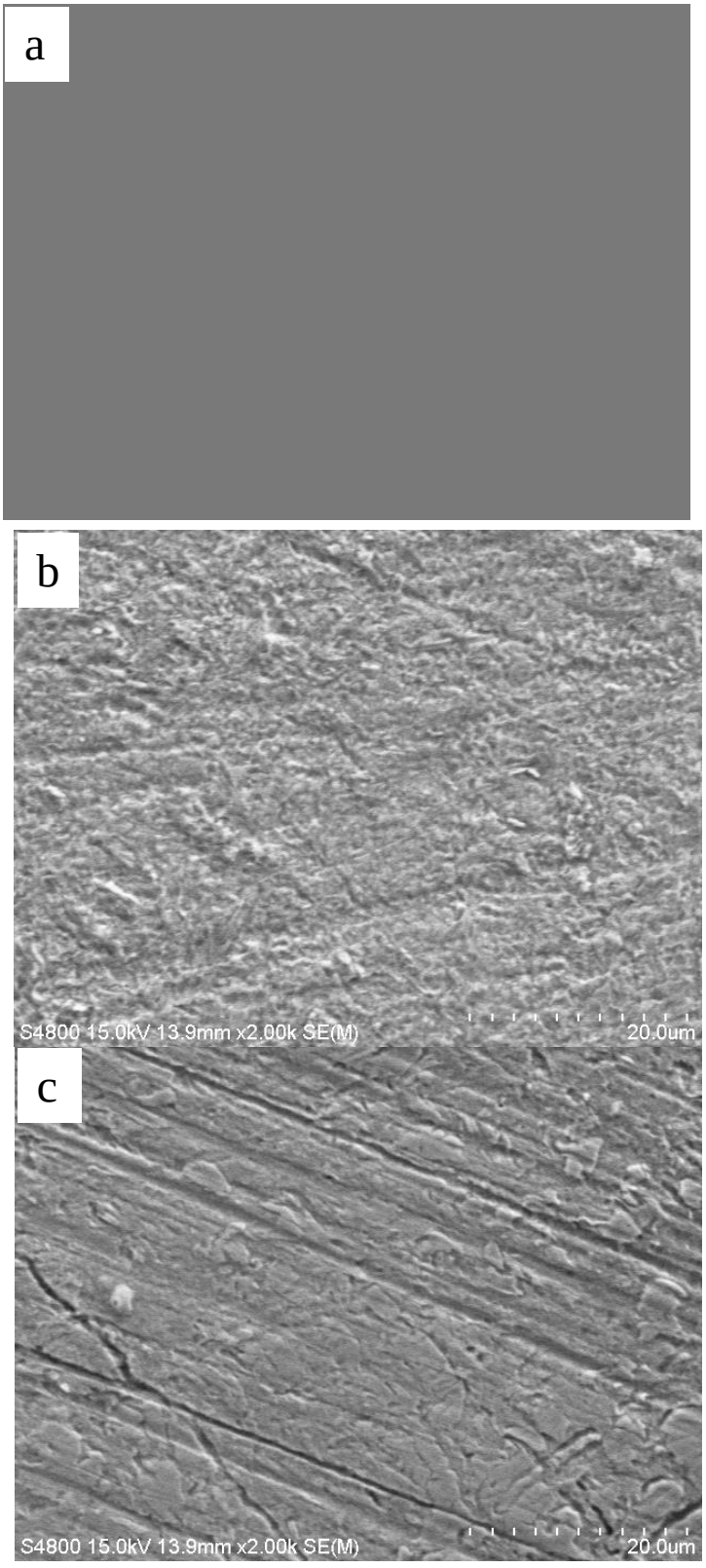

Figure 8. SEM micrographs of carbon steel sheets without immersion in any corrosive solution(a), suspension in blank 1.0 M HCl solution (b) and immersion in 1.0 M HCl solution with 40 mg L^{-1} dppy (c).

In comparison with the carbon steel surface immersed in the blank 1.0 M HCl solution, the carbon steel surface suspended in HCl solution with 40 mg L^{-1} dppy (Figure 8c) was relatively smoother with fewer pits. This indicates that dppy drastically decreased the corrosion of carbon steel in blank 1.0 M HCl medium. The excellent corrosion inhibition is ascribed to two factors: first, the surface of carbon steel is covered by a more compact and less porous dppy film acting as a barrier to prevent the corrosive solution from reaching the metal surface; second, a large poly(styrene sulfonate) anion with a long hydrophobic group is accumulated at the interface between the dppy film and metal to react with the cation to form a protective insoluble compound to further contribute to the corrosion inhibition effect.

4. CONCLUSIONS

Doped polypyrrol (dppy) was synthesized and analyzed as a corrosion inhibitor for carbon steel in 1.0 M HCl media by weight loss technique, electrochemical method and SEM observation. The main points of this work can be drawn as follows:

1. Doped polypyrrol (dppy) is a promising corrosion inhibitor for carbon steel in 1.0 M HCl media.

2. The corrosion inhibitive efficiency is enhanced by an increment in the dppy concentration and temperature. The high value of corrosion inhibitive efficiency is 87.1% at 40 mg L^{-1} (333 K) from the weight loss results.

3. The adsorption of dppy molecules on the carbon steel surface is a mixed-type adsorption dominated by chemisorption. In the experimental temperature range, the adsorption of dppy on carbon steel conforms to the Langmuir adsorption isotherm, and it is a spontaneous, endothermic adsorption process with an increase in entropy.

4. Electrochemical impedance spectroscopy results suggest an increment in charge transfer resistance and a reduction in double layer capacitance with increasing concentration of dppy resulted from the displacement of water molecules by dppy molecules.

5. Potentiodynamic polarization data indicate that dppy behaves as a mixed-type corrosion inhibitor retarding both anodic carbon steel oxidation and cathodic hydrogen ion reduction reactions simultaneously.

ACKNOWLEDGEMENTS

The authors gratefully acknowledge the financial and experimental support received from the Liaoning Provincial Department of Education and Shenyang Jianzhu University for supporting this work by Grant No (LJZ2017038) and (2017046).

References

1. X. M. Wang, H. Y. Yang, F. H. Wang, *Corros. Sci.*, 55 (2012) 145–152.
2. E. Khamis, M. Atea, *Corrosion*, 8 (1994) 106–112.

3. H. Keleş, Mustafa Keleş, İ. Dehri, O. Serindağ, *Mater. Chem. Phys*., 112 (2008) 173–179.
4. R. Farahati, A. Ghaffrainejad, S. M. Mousavi-Khoshdel, J.Rezania, H.Behzadi, A. Shockravi *Prog. Org. Coat.*, 132(2019) 417-428.
5. 5.. T. Zhou, J. Yuan, Z. Q. Zhang, X. Xin, G.Y. Xu, *Colloids Surf. A: Physicochem. Eng.Aspects*, 575(2019) 57-65.
6. C. Monticelli, A.Balbo, J. Esvan, C. Chiavari, C. Martini, F. Zanotto, L.Marvelli, L. Robbiola, *Corros. Sci*., 148(2019) 144-158.
7. C. M. Fernandes, L. X. Alvare, N. E. Santos, A. C. M. Barrios, E. A. Ponzio, *Corros. Sci*., 149 (2019) 185–194.
8. R. S. Erami, M. Amirnasr, S. Meghdadi, M. Talebian, H. Farrokhpour, K. Raeissi, *Corros. Sci.*, 151 (2019) 190–197.
9. M. Morad, A. El-Dean, *Corros. Sci.*, 48 (2006) 3398–3412.
10. R. Solmaz, E. AltunbaŞ, G. KardaŞ, *Mater. Chem. Phys*., 125 (2011) 796–801.
11. B. M. Mistry, S. K. Sahoo, S. Jauhari, *J. Electroanal. Chem.*, 704 (2013) 118–129.
12. H. KeleŞ, M. KeleŞ, I. Dehri, O. Serindağ, *Coll. Surf. A Physicochem. Eng. Asp*., 320 (2008) 138–145.
13. H. KeleŞ, M. KeleŞ, I. Dehri, O. Serindağ, *Mater. Chem. Phys*., 112 (2008) 173–179.
14. C. Verma, I. B. Obot, I.Bahadur, El-Sayed M.Sherif, E. E.Ebenso, *Appl. Surf. Sci*., 457 (2018) 134–149.
15. K. F. Khaled, M. A. Amin, *Corros. Sci*., 51 (2009) 1964–1975.
16. Y. H. Lei, N. Sheng, A. Hyono, M. Ueda, T. Ohtsuka, *Prog. Org. Coat.*, 77 (2014) 774–784.
17. A. El Jaouhari , M. Laabd, E. A. Bazzaoui, A. Albourine, J. I. Martins, R. Wang, G. Nagy, M. Bazzaoui, *Synthetic Met.*, 209 (2015) 11–18.
18. Y. J. Ren, J. Chen, C. L. Zeng, C. Li, J. J. He, *Int. J. Hydrogen Energ*., 41 (2016) 8542-8549.
19. A. Omrani, H. Rostami, R. Minaee, *Prog. Org. Coat*., 90 (2016) 331–338.
20. L. L. Zhang, S. J. Liu, H. C. Han, Y. Zhou, S. C. Hu, C. He, Q. X. Yan, *Surf. Coat. Tech*., 341 (2018) 95–102.
21. M. Hosseini , L. Fotouhi, Ali Ehsani, M. Naseri, *J. Colloid Interf. Sci*., 505 (2017) 213–219.
22. M. Saremi, M. Yeganeh, *Corros. Sci*., 86 (2014) 159–170.
23. M. Bouklah, N. Benchat, B. Hammouti, A. Aouniti, S. Kertit, *Mater. Lett*., 60 (2005) 1901–1905.
24. L. Guo, G. Ye, I. B. Obot, X. Li, X. Shen, W. Shi, X. Zheng, *Int. J. Electrochem. Sci*., 12 (2017) 166–177.
25. D. S. Chauhan, K. R. Ansari, A. A. Sorour, M. A. Quraishi, H. Lgaz, R.Salghi, *Int. J. Biol. Macromol.*, 107 (2018) 1747–1757.
26. M. Prabakaran, S. H. Kim, V. Hemapriya, I. M. Chung, *Res.Chem. Intermed*., 42 (2016) 3703–3719.
27. A. Saxena, D.Prasad, R. Haldhar, G. Singh, A. Kumar, *J. Environ. Chem. Eng.*, 6 (2018) 694–700.
28. R. Menaka, S. Subhashini, *J. Adhes. Sci. Technol*., 30 (2016) 1622-1640.
29. Y. Peng, A. E. Hughes, G. B. Deacon, P. C. Junk, B. R.W.Hinton, M. Forsyth, J. I. Mardel, *Corros.Sci.*, 145 (2018) 199-211.
30. A. Y. Adesina, Z. M. Gasem, A. Madhan Kumar, *Metall. Mater. Trans. B Process Metall. Mater. Process. Sci*., 48 (2017) 1–12.
31. A. K. Singh, E. E. Ebenso, M. A. Quraishi, *Res. Chem. Intermed*., 39 (2013) 3033–3042.
32. M. Larif, A. Elmidaoui, A. Zarrouk, H. Zarrok, R. Salghi, B. Hammouti, H. Oudda, F. Bentiss, *Res. Chem. Intermed.*, 39 (2013) 2663–2677.
33. Y. Yan, W. H. Li, L. K. Cai, *Electrochimica Acta*, 53 (2008) 5953-5960.
34. F. L. Xu, J. Z. Duan, S. F. Zhang, *Mater. Lett*., 62 (2008) 4072-4074.
35. D. K. Yadav, M. A. Quraishi, B. Maiti, *Corros. Sci*., 55 (2012) 254–266.
36. I. B. Obot, I. B. Onyeachu, A. M. Kumar, *Carbohydr. Polym*., 178 (2017) 200-208.
37. N. Dang, Y. H. Wei, L. F. Hou, Y. G. Li, C. L. Guo, *Mater. Corros*., 66 (2015) 1354-1362.

38. S. M. Tawfik, *RSC Adv*., 5 (2015) 104535-104550.
39. S. S. A. El-Rehim, A. M. M. Ibrahim, K. F. Khaled, *J. Appl. Electrochem*., 29 (1999) 593-599.
40. E. Patricia, M. Alvarez, V. Fiori-Bimbi , A. Neske, A. S. Brandán, A. C. Gervasi, *J. Ind. Eng. Chem.*, 58 (2018) 92–99.
41. H. Ashassi-Sorkhabi, M. R. Majidi, K. Seyyedi, *Appl. Surf. Sci*., 225(2004) 176-185.
42. X. M. Wang, H. Y. Yang, F. H. Wang, *Corros. Sci.*, 52 (2010) 1268–1276.
43. N. A. Odewumni, S. A. Umoren, Z. M. Gasem, *J. Ind. Eng.Chem*., 21 (2014) 239–247.
44. K. P. V. Kumar, M. S. N. Pillai, G. R. Thusnavis, *J. Mater. Sci. Technol*., 27 (2011) 1143–1149.
45. M. Chevalier, F. Robert, N. Amusant, M. Traisnel, C. Roos, M. Lebrini, *Electrochim. Acta*, 131 (2014) 96–105.
46. A. Asan, M. Kabasakaloglu, M. I. siklan, *Corros. Sci*., 47 (2005) 1534-1544.
47. R. Yildiz, T. Dogan, I. Dehri, *Corros. Sci*., 85 (2014) 215–221.
48. Z. H. Tao, Z. S. Tao, W. H. Li, *Corros. Sci*., 51 (2009) 2588-2595.
49. A. M. Al-Sabagh, M. A. Migahed, H. S. Awad, *Corros. Sci*., 48 (2006) 813-828.
50. K. K. Anupama, K. Ramya, K. M. Shainy, Abraham Joseph, *Mater.Chem. Phys*., 167 (2015) 28-41.
51. F.S. de Souza, A. Spinelli, *Corros. Sci.* 51 (2009) 642-649.
52. S. A. Umoren, I. B. Obot, E. E. Ebenso, *Eur. J. Chem*., 5 (2008) 355-364.
53. F. Bentiss, M. Lebrini, M. Lagrenee, *Corros. Sci*., 47 (2005) 2915-2931.
54. E. A. Noor., A. H. Al-Moubaraki, *Mater. Chem. Phys*., 110 (2008) 145-154.
55. M. A. Bedair, M.M.B. El-Sabbah , A.S. Fouda , H. M. Elaryian, M. A. Bedair, M. M. B. El-Sabbah, A. S. Fouda, H. M. Elaryian, *Corros. Sci.*, 128 (2017) 54–72.
56. C. Jing, Z. Q. Wang, Y. L. Gong, H. J. Huang, Y. W. Ma, H. X. Xie, H. R. Li, S. T. Zhang, F. Gao, *Corros. Sci*., 138 (2018) 353-371.
57. T. P. Zhao, G. N. Mu, *Corros. Sci.*, 41 (1999) 1937–1944.